International Journal of New Technology and Research (IJNTR)
ISSN:2454-4116, Volume-4, Issue-3, March 2018 Pages 15-20

Extended Contrast Local Binary Pattern for Texture Classification

Jie Sima, Yongsheng Dong*, Tianyu Wang, Lintao Zheng , Jiexin Pu

***Abstract*—Considering the limitation that LBP only focuses on the sign feature in extracting the texture feature as well as its low recognition rate, we in this paper propose an extended contrast ratio local binary pattern for texture classification. The extracted features include its sign feature, energy feature and its center pixel feature, which aims at constructing the histogram based on the features of the sign energy center pixel gained before. Then we perform texture classification by employing the Chi-square distance and the nearest neighbor classifier. Experimental results reveal that our proposed method outperforms several representative texture classification methods.**

***Index Terms*—Feature extraction, Energy feature, Local multi-values pattern, Global information, Rotational invariance.**

I. INTRODUCTION

The importance of texture in the pattern recognition and graphic information processing needs no emphasis. Therefore, texture feature extraction is regarded as the focus and basis of texture study, analysis and application. Studies on feature extraction and texture classification has gained extensive attention by numerous scholars, which has been widely applied in areas like facial recognition [1-3], medical biology analysis [4] and license plate number detection [5, 6].

In the past 50 years, large numbers of methods on how to effectively extract the texture feature has been put forward by worldwide scholars[7, 8]. These methods can be divided into four categories to our present study: statistic method [9-11], structure-based method [12-16], model-based method [17-19] and transform-based [20-22]. All these derived algorithms mentioned above have gained widely study and practice for its good performance and computational simplicity , yet they are still to be improved for the following deficiencies. First, most of them ignore the global energy information of an image. Second, they lack the consideration of the magnitude and quantity of bins during the constructing process of the feature histogram. Third, there still exists high rate of inaccuracy in extracting the center pixel feature.

Jie Sima, School of Information Engineering, Henan University of Science and Technology, Louyang 471023, Henan, P. R. China

Yongsheng Dong,(corresponding author) School of Information Engineering, Henan University of Science and Technology, Louyang 471023, Henan, P. R. China

Tianyu Wang, School of Information Engineering, Henan University of Science and Technology, Louyang 471023, Henan, P. R. China.

Lintao Zheng, School of Information Engineering, Henan University of Science and Technology, Louyang 471023, Henan, P. R. China.

Jiexin Pu, School of Information Engineering, Henan University of Science and Technology, Louyang 471023, Henan, P. R. China.

In view of the inefficiencies above, this paper presents the extended contrast local binary pattern (ECLBP). This pattern contains three parts to be accomplished, including the center pixel local binary pattern, contrast ratio difference energy, The first part is the Sign Feature Extraction (SFE); The second part, Contrast Difference Energy Feature (CDEF) not only extracts the energy feature through the contrast ratio between the pixels, but also constructs a histogram from small to large according to the interval value. And, Extension Center Pixel Feature (ECPF) serves to expand binary pattern, set the parameter and converts the graphic into multiple value.

The contributions of the method made in this paper lie in the following points: First, we construct a new way to divide the bins, which in turn elevates the accuracy rate of feature extraction. Second, we convert the original binary value into multiple value in order to represent the image feature by changing the parameter. Finally, experimental results on typical texture datasets reveal that our proposed method outperforms several representative texture classification methods.

The next organization of this paper as follows. The related works are introduced in section 2. Section 3 describes our proposed method. Section 4 presents our experimental setting and experimental results. Finally, Section 5 is a brief summary.

II. RELATED WORK

As a perceived form of how human visual system reacts towards the surface of the object, the textural feature resembles and reflects the properties of the image itself. The texture feature differentiate itself from other image feature such as gray scale or color, it displays the variation of the gray-scale of one pixel and other adjacent pixels in an image as well as the disciplinarian distribution of light-intensity. It serves to demonstrate the roughness and orientation of the surface of an object as well as whether the surface of an object conforms to certain rule. The global texture information is formed by the different degree of local texture information.

Texture feature extraction are mainly divided into two categories: spatial domain methods, transform domain methods. Spatial analysis methods are based on the correlation between spatial pixels and their neighborhood pixels, suitable for rotating image texture feature description. Transform domain methods are the use of transform coefficients for image analysis, suitable for non rotation image texture feature description.

The local binary pattern (LBP) [23] put forward by Ojala in

2002 has won extensive appreciation owing to its low complexity, rotation invariance, insensitivity of the illumination variation and its easiness to be comprehended. Thus, amounts of derived LBP algorithm started to appear, such as dominant LBP (DLBP) [24], completed LBP (CLBP) [25, 26], local ternary pattern (LTP) [27, 28], local binary count (LBC) [29]. Among these algorithms, DLBP takes the pattern feature as the main consideration; CLBP is represented based on the center pixel and the local difference sign-magnitude transform, while LTP classifies the positive pattern from the negative pattern by altering the threshold.The next two chapters will briefly review the completed local binary pattern (CLBP), local ternary pattern(LTP)[32].

A. *Completed Local Binary Pattern (CLBP)*

When the texture features of the LBP is extracted, a part of the information is lost, so that the same results can be obtained for different structures. Figure 2.1 shows the same binary string of two different structures obtained after the threshold.

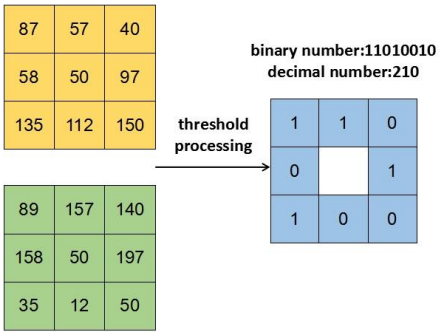

Figure 2.1 LBP with Different Structures

Therefore, Guo et al. Proposed a complete LBP operator consists of two parts, namely, CLBP_Center (CLBP_C) and the local difference sign-magnitude (LDSMT). The local difference sign-magnitude is divided into the CLBP-Sign (CLBP_S) and the CLBP-Magnitude (CLBP_M), as shown in Figure 2.2

CLBP_Center (CLBP_C) is defined as

$$CLBP\_C_{P,R} = t(g_c * c)$$

$$t(x,c) = \begin{cases} 1 & x \geq c \\ 0 & else \end{cases} \tag{2.1}$$

The local difference sign-magnitude (LDSMT) is shown as follows. The sign of a is represented by B, and the value is represented by C.

$$d_p = s_p * m_p$$

$$m_p = |d_p|, s_p = \begin{cases} 1 & d_p \geq 0 \\ -1 & d_p < 0 \end{cases} \tag{2.2}$$

CLBP-Magnitude (CLBP_M) is defined as

$$CLBP\_M_{P,R} = \sum_{P=0}^{P-1} s(m_p - c)2^p \tag{2.3}$$

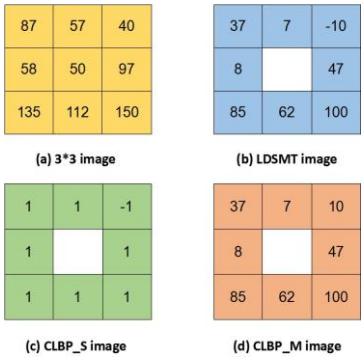

Figure 2.2 CLBP

B. *Local ternary pattern(LTP)*

LTP is the derivative algorithm of LBP, the principle is a length of 2t open interval [-t, t]. If the difference between the neighborhood pixel gray value g and the center pixel value g lies in the right side of the interval, the input value is encoded as 1. If the difference falls the left side of the interval, the input value is encoded as -1. If the difference lies in the interval , the input value is encoded as 0. The formula is as follows.

$$s(x, g_c, t) = \begin{cases} 1 & x \geq g_c + t \\ 0 & |x - g_c| < t \\ -1 & x \leq g_c - t \end{cases} \tag{2.4}$$

LTP to some extent resist the impact of noise and enhance the description of the texture. Which t is worth setting is particularly important. The schematic diagram is shown in Figure 2.3.

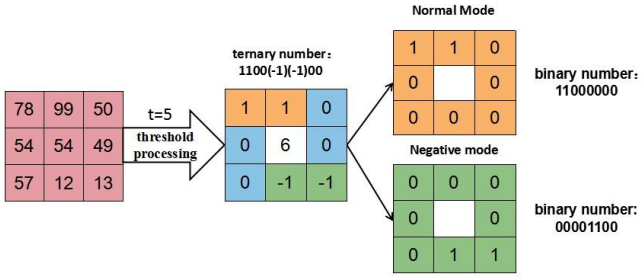

Figure 2.3 LTP algorithm

III. Extended Contrast Local Binary Pattern (ECLBP)

This paper presents the extended contrast local binary pattern (ECLBP). The texture feature which is extracted from the image texture representation method consists of the following three parts. This pattern contains three parts to be accomplished, including the center pixel local binary pattern, contrast ratio difference energy, The first part is the Sign Feature Extraction (SFE), which is the Original LBP; The second part, Contrast Difference Energy Feature (CDEF) not only extracts the energy feature through the contrast ratio between the pixels, but also constructs a histogram from small to large according to the interval value. And, Extension Center Pixel Feature (ECPF) serves to expand binary pattern, set the parameter and converts the graphic into multiple value.

We extract features from the image in the three methods, and the three texture features as the image of the texture features. Figure 3.1 shows the overall flow chart of our

approach.

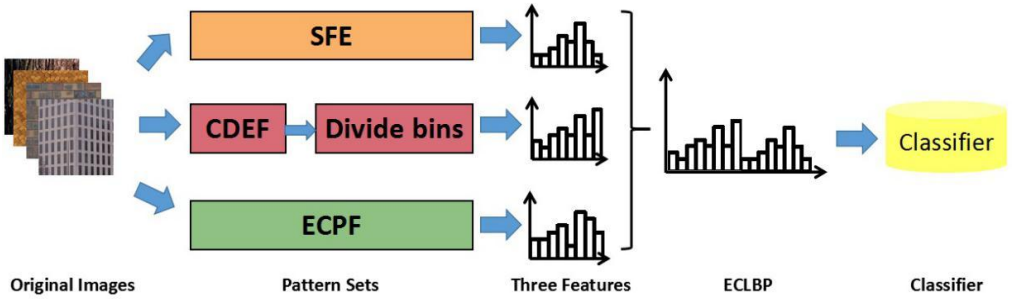

Figure 3.1 The flow chart of the proposed texture classification method

A. Sign Feature Extraction (SFE)

Conventional LBP is mainly employed in sign feature extraction. It extracts the valid texture feature to measure and describe the different image texture information and eventually to represent the space structure and sign information of the local texture image. The patch in an LBP can be randomly extended to its neighbors. The common (P,R) is to define a (3*3) patch, choose one pixel as the center pixel and contrast the value of the center pixel and its eight neighbors. 0 is to be used when it is below the center pixel, 1 when it equals or is above the center pixel. Then get a 01 string of LBP patterns in a fixed direction. The string multiplied by weight of corresponding pixels, and then this value is the LBP value of the center pixel. If g_c is to represent center pixel, g_p the value of its neighbors, then the LBP code can be defined as:

$$LBP_{P,R} = \sum_{P=0}^{P-1} s(g_p - g_c)2^P, s(x) = \begin{cases} 1, x \geq 0 \\ 0, x < 0 \end{cases} \quad (3.1)$$

For $LBP_{P,R}$, it produces 2^p different output values ranging from 0 to 1., while another equivalent patter $LBP^{u2}_{P,R}$ form the binary pattern into a circular chain, While $U(G_p)$ stands for the transitions to or from 0 to 1.

$$U(G_P) = \left|s(g_{p-1} - g_c) - s(g_i - g_c)\right| + \sum_{P=1}^{P-1} \left|s(g_p - g_c) - s(g_{p-1} - g_c)\right| \quad (3.2)$$

When the former pattern is rotated, another rotation invariant equivalent can be used, which decreases the total possible pattern amount from 2^p to p+1. All these equivalences are classified into the P+1 the pattern as is shown in the following:

$$LBP^{riu2}_{P,R} = \begin{cases} \sum_{P=0}^{P-1} s(g_p - g_c) & U(G_p) \leq 2 \\ P+1 & U(G_p) > 2 \end{cases} \quad (3.3)$$

And the $LBP_{P,R}$ histogram of the image f(x,y) can be defined as :

$$H_i = \sum_{x,y} I(f(x,y), i), i = 0,1,...,n-1$$
$$I(x,y) = \begin{cases} 1 & x = y \\ 0 & otherwise \end{cases} \quad (3.4)$$

B. Contrast Difference Energy Feature (CDEF)

Considering the fact that conventional LBP ignores the global energy information, therefore, a contrast difference energy feature is purposed in this chapter, which implements the energy information of the image. The LBP can be extended to its neighbors. The common (P, R) is to define a (3*3) patch, choose one pixel as the center pixel and contrast the difference value of the center pixel and its eight neighbors. The difference value is used to get the mean value after seeking its square. If g_c is to represent the center pixel, g_p is the neighbor pixel of g_c, then the CDEF code can be represented as :

$$CDEF = \frac{1}{P} \sum_{P=0}^{P-1} (g_P - g_c)^2 \quad (3.5)$$

Then it becomes especially important to choose an appropriate bins when constructing the feature histogram. Considering that CDEF aims at getting the difference value of the pixel and its neighbors, which is relatively small, therefore, we choose to construct the bins from small to large rather than use equal interval when constructing the contrast ratio difference energy feature histogram. Setting FD as a difference value, min represents the minimum of the image pixel, while max the maximum.

$$FD = \frac{\max - \min}{10} \quad (3.5)$$

Setting a new interval CV, and we get 13 critical value through the text $CV_0, CV_1 ... CV_{12}$. When 0 ⩽ i<10, H(x)=FD/11, FD/10...FD/2; while H(x)=FD*1, FD*2, FD*3, when 10⩽i⩽12.

$$CV_i = H(x) + \min, \quad i \in [0,12] \quad (3.6)$$

$$H(x)=\begin{cases} FD*j^{-1} & 0\le i<10 \quad j\in 11,10,...,2 \\ FD*t & 10\le i\le 12 \quad t\in 1,2,3 \end{cases} \tag{3.7}$$

Setting j=11, t=3, after setting the critical value, the interval of the histogram can be divided into the Figure 3.2:

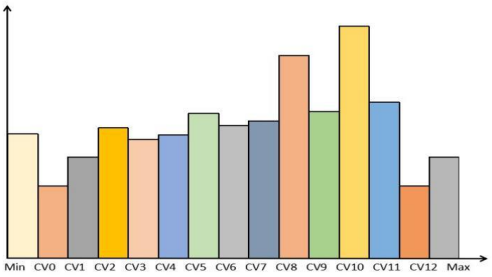

Figure 3.2 The divide of the bins

C. *Extension Center Pixel Feature (ECPF)*

During the extraction of the image feature, this method employs multiple value rather than binaryzation. It alters the parameter during the test, in order to obtain the multiple value and to represent the image feature. According to the test, it proves that the test result turns to be most satisfactory when the parameter sets12. For example, Figure 3.3 shows which we define a 3*3 patch and then get the reminders after the value is divided by 12, the code is defined as follows:

Figure 3.3 ECPF algorithm

IV. Experimental Results

In this chapter, in order to prove the performance of the extension contrast ratio local binary pattern, we calculate the accuracy rate of classification on five texture sets. On each texture set, ten test samples and classification samples are randomly selected for experiment, and the average of ten results is taken as the final accuracy rate of classification.

The next section proposes similarity measurement and parameter settings, after which the classification accuracy and time-consuming of each texture set are given.

A. *Similarity Measurement*

In statistical pattern recognition, there are many metric formulas for measuring similarity between features, such as Mahalanobis distance, Euclidean distance, and chi square distance. Although they have different representations, these distance formulas have the same goal, that is, the degree of similarity between the two features can be well calculated.

In this paper, we employ the nearest neighbor classifier and chi square distance to calculate the distance from a test sample to a training sample. At the stage of the classification test, we calculate the distance between each test sample and all the training samples. The test samples are classified into a minimum distance with training samples.

The following formula is used to calculate the distance. We represents the total number of the feature histogram bins, and φ stands for the number of all training samples.

$$D_i=\sum_{j=1}^{W}\frac{(F_{te}^{j}-F_{tr}^{i,j})^2}{(F_{te}^{j}+F^{i,j}_{tr})},i=1,2,...,\varphi, \tag{4.1}$$

where F_{te}^{j} is the j-th bin of the feature histogram of a test sample, $F_{tr}^{i,j}$ is the j -th bin of the feature histogram of the i-th training sample. When a classification experiment is conducted, a test sample is assigned to the category to which the training sample is closest to the training sample.

B. *Texture Datasets*

To comprehensively evaluate our proposed method, we conducted a series of experiments on a powerful databases and three experimental samples from the texture datasets is chosen: the Brodatz database, which contains 111 different texture classes, and each class has a 640*640 image.

In our experiments, we take the central region of each image of 320*320 as the experimental image. In order to verify the rotation invariance of the method, we rotate each class clockwise, 5 degrees, 10 degrees, 30 degrees, 45 degrees, 60 degrees, 75 degrees, 90 degrees, as shown in Figure 4.1. And then split the rotated image into four experimental samples. For the three subsets, each class is divided into 32 160*160 experimental samples, half samples of each class are randomly selected for training and the rest is used for testing. These three datasets contain 960, 1920 and 3552 experimental samples, respectively.

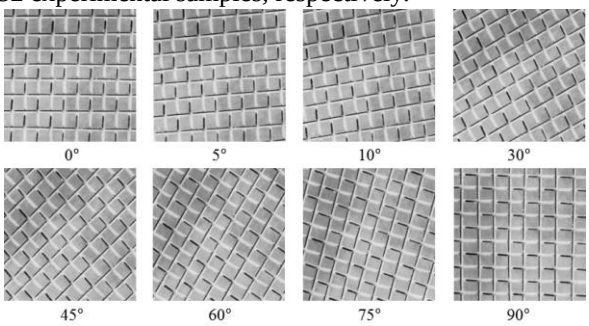

Figure 4.1 A class that rotates clockwise at eight angles

Set-1: We randomly selected 30 images from Brodatz as our Set-1 experimental data and validate the rotational invariance of our approach on it, as shown in Figure 4.2. The 30 photos of Brodatz album. The sequence is arranged from left to right and top to bottom: D1, D3, D8, D10, D11, D13, D17, D19, D21, D23, D25, D29, D31, D33, D34, D35, D45, D46, D50, D55, D63, D64, D73, D75, D94, D95, D100, D103, D105 and D111.

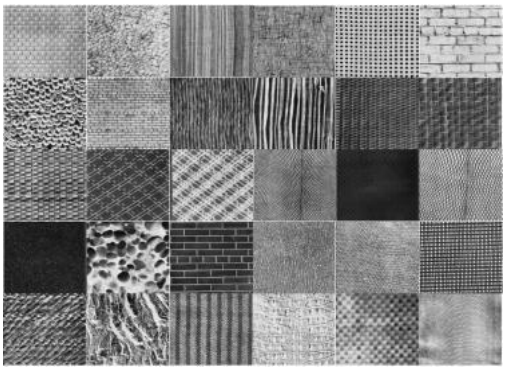

Figure 4.2 The 30 texture images in Set-1

Set-2: We randomly selected 60 images from Brodatz, as

shown in Figure 4.3. The sequence is arranged from left to right and top to bottom: D2, D3, D4, D5, D6, D8, D12, D18, D20, D21, D23, D24, D27, D28, D30, D32, D33, D36, D37, D38, D39, D40, D43, D45, D46, D47, D48, D50, D51, D52, D53, D58, D61, D63, D64, D65, D67, D69, D70, D73, D74, D75, D77, D78, D79, D81, D83, D85, D86, D87, D88, D91, D92, D94, D95, D96, D102, D105, D107 and D108.

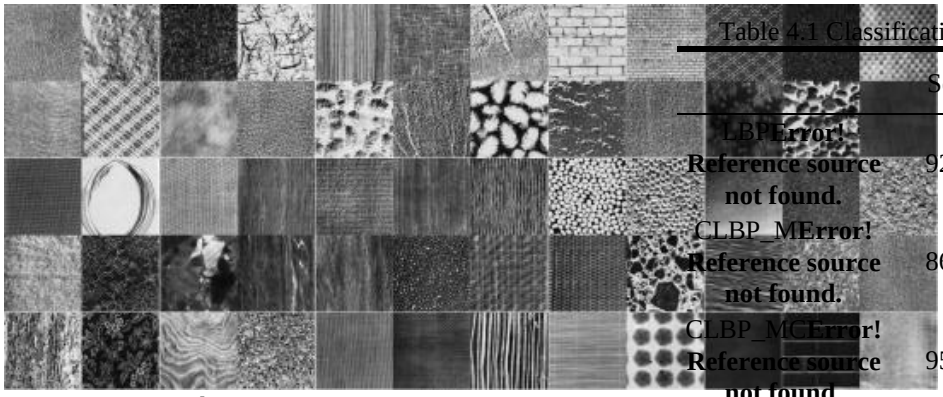

Figure 4.3 The 60 texture images in Set-2
Set-3: Set-3 is the whole Brodatz database.

C. Parameter Setting

In our approach, we set the two parameters through the experiment Set-1, Set-2, Set-3, which enables us to get the optimized performance and the highest classification rate.

Through experiments we can get the optimal parameters of CV in ECDF, When $0 \leqslant i<10$, H(x)=FD/11, FD/10, ...FD/2; while H(x)=FD*1, FD*2, FD*3 when $10 \leqslant i \leqslant 12$. and Another parameter results are shown in Figure 4.4. From the Figure 4.4, we could get the highest classification rate when 18 is set as the critical value.

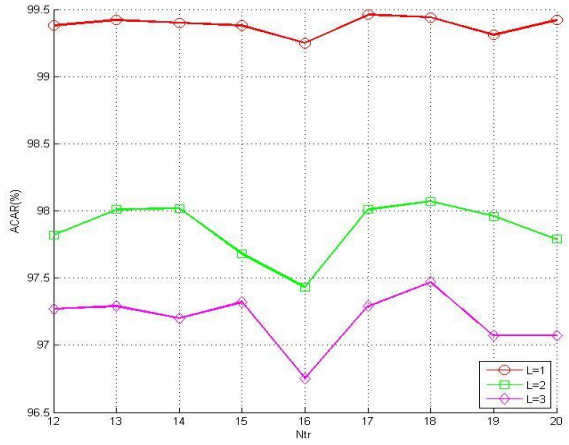

Figure 4.4 Parameter setting

D. Classification Performance and Comparisons

In this section, we conduct two experiments to evaluate our proposed method. The first one is to verify the rotation invariance, while the second is to contrast its classification rate with the rest method.

To verify the effectiveness of our proposed method, we compare it with eight representative methods LBP[23], CLBP_M [25], CLBP_MC[25], CLBP_S_MC[25], CLBP_SM[25], CLBP_SMC[25], PMC-BC[30], and LRS-MD[31]. We report the classification results of the nine methods in Table 1. It can be seen from Table 1 that our proposed method is competitive, and outperforms CLBP_SMC and PMC-BC by over 3.00%. The experimental results shown in table.

Table 4.1 Classification results of the comparative methods: LBP, CLBP_M, CLBP_MC, CLBP_S_MC, CLBP_SM, CLBP_SMC, PMC-BC, LRS-MD and our proposed ECLBP.

Table 4.1 Classification results of the nine methods

	Set-1	Set-2	Set-3
LBP**Error! Reference source not found.**	92.27	92.56	97.27
CLBP_M**Error! Reference source not found.**	86.23	92.39	96.31
CLBP_MC**Error! Reference source not found.**	95.76	97.98	99.23
CLBP_S_MC**Error! Reference source not found.**	96.65	98.54	99.56
CLBP_SM**Error! Reference source not found.**	99.33	98.88	97.96
CLBP_SMC**Error! Reference source not found.**	99.71	99.51	98.56
PMC-BC[30]	95.73	93.44	86.36
LRS-MD**Error! Reference source not found.**	93.19	89.16	80.46
ECLBP	99.63	98.51	98.13

E. Computational costs

In this paper, all experiments have been implemented on a workstation with Intel Core E5 central processing unit (1.70 GHz) and 4-G random access memory in the MATLAB environment. Table shows the running time of each method on Set-1, Set-2. It can be seen, LBP time to spend the least.

Table 4.2 The computational costs of the comparative methods: LBP, CLBP_M, CLBP_MC, CLBP_S_MC, CLBP_SM, CLBP_SMC, PMC-BC, LRS-MD and our proposed ECLBP

Table 4.2 The computational costs of the nine methods

	Set-1	Set-2
LBP**Error! Reference source not found.**	26.21	58.28
CLBP_M**Error! Reference source not found.**	29.43	58.09
CLBP_MC**Error! Reference source not found.**	25.41	57.89
CLBP_S_MC**Error! Reference**	27.96	60.50

source not found.		
CLBP_SM**Error! Reference source not found.**	30.59	58.44
PMC-BC[30]	848.98	1673.06
LRS-MD**Error! Reference source not found.**	489.48	964.32
ECLBP	29.84	68.50

V. Conclusion

In this paper, we propose an extended contrast local binary pattern for texture classification. It is implemented by performing the contrast between pixels to get the energy feature of images, which was usually ignored by conventional LBP. Besides, we construct a feature histogram with the bins from small to large based on the feature of the images. Finally, we extend the binary pattern and set the parameter to improve the correct extraction rate. Experimental results show that our proposed method is effective when comparing it with several representative methods.

References

[1] H. M. Takallou and S. Kasaei, "Multiview face recognition based on multilinear decomposition and pose manifold," IET Image Processing, vol. 8, no. 5, pp. 300 - 309, 2014.

[2] H. Zheng, Q. Ye and Z. Jin, "A novel multiple kernel sparse representation based classification for face recognition," KSII Transactions on Internet and Information Systems, vol. 8, no. 4, pp. 1463-1480, 2014.

[3] Z. Liu, C. Yang, J. Pu, G. Liu and S. Liu, "Robust minimum squared error classification algorithm with applications to face recognition," KSII Transactions on Internet and Information Systems, vol. 10, no. 1, pp. 308-320, 2016.

[4] S. Shahbeig, "Automatic and quick blood vessels extraction algorithm in retinal images," IET Image Processing, vol. 7, no. 4, pp. 392 - 400, 2013.

[5] M. Varma and A. Zisserman, "A statistical approach to material classification using image patches," IEEE Transactions on Pattern Analysis and Machine Intelligence, vol. 31, no. 11, pp. 2032 - 2047, 2009.

[6] K. S. Dash, N. B. Puhan and G. Panda, "Handwritten numeral recognition using non-redundant stockwell transform and bio-inspired optimal zoning," IET Image Processing, vol. 9, no. 10, pp. 874 - 882, 2015.

[7] K. H. Oh, S. H. Kim, Y. C. Kim and Y. R. Lee, "Detection of multiple salient objects by categorizing regional features," KSII Transactions on Internet and Information Systems, vol. 10, no. 1, pp. 272-287, 2016.

[8] F. Yuan, J. Shi, X. Xia, Y. Yang, Y. Fang and R. Wang, "Sub oriented histograms of local binary patterns for smoke detection and texture classification," KSII Transactions on Internet and Information Systems, vol. 10, no. 4, pp. 1807-1823, 2016.

[9] S. K. Choy and C. Tong, "Statistical properties of bit-plane probability model and its application in supervised texture classification," IEEE Transactions on Image Processing, vol. 17, no. 8, pp.1399 - 1405, 2008.

[10] M. Varma and A. Zissermann, "A statistical approach to texture classification from single images," International journal of computer vision, vol. 62, no. 1(2), pp. 61 - 81, 2005.

[11] Y. Ma, L. Liu, K. Zhan and Y. Wu, "Pulse coupled neural networks and one-class support vector machines for geometry invariant texture retrieval," Image and vision computing, vol. 28, no. 11, pp. 1524 - 1529, 2010.

[12] X. Qi, R. Xiao, C. Li, Y. Qiao, J. Guo and X. Tang, "Pairwise rotation invariant co-occurrence local binary pattern," IEEE Transactions on Pattern Analysis and Machine Intelligence, vol. 36, no. 11, pp. 2199 - 2213, 2014.

[13] L. Nanni, S. Brahnam and A. Lumini, "A simple method for improving local binary patterns by considering nonuniform patterns," Pattern Recogn, vol. 45, no. 11, pp. 3844 - 3852, 2012.

[14] X. Qian, X. Hua, P. Chen, and L. Ke, "PLBP: an effective local binary patterns texture descriptor with pyramid representation," Pattern Recogn, vol. 44, no. 10(11), pp. 2502 - 2515, 2011.

[15] Z. Guo, L. Zhang and D. Zhang, "Rotation invariant texture classification using LBP variance (LBPV) with global matching," Pattern Recogn, pp. 706 - 719, 2010.

[16] Y. Zhao, D. Huang, and W. Jia, "Completed local binary count for rotation invariant texture classification," IEEE Transactions on Image Processing, vol. 21, no. 21(10), pp. 4492 - 4497, 2012.

[17] H. Lategahn, S. Gross, T. Stsehle and T. Aach, "Texture classification by modeling joint distributions of local patterns with gaussian mixtures," IEEE Transactions on Image Processing, vol. 19, no. 6, pp. 1548 - 1557, 2010.

[18] F. Perronnin and C. Dance, "Fisher kernels on visual vocabularies for image categorization," IEEE conference on computer vision and pattern recognition, pp. 1 - 8, 2007.

[19] S. Lazebnik, C. Schmid and J. Ponce, "A sparse texture representation using local affine region," IEEE Transactions on Pattern Analysis and Machine Intelligence, vol. 27, no. 8, pp. 1265 - 1278, 2005.

[20] Y. Dong and J. Ma, "Texture classification based on contourlet subband clustering," in Proc. of 7th Int. Conf. Intell. Comput., Zhengzhou, China, PP. 421 - 426, 2011.

[21] C. M. Pun and M. C. Lee, "Log-polar wavelet energys ignatures for rotation and scale invariant texture classification," IEEE Transactions on Pattern Analysis and Machine Intelligence, vol. 25, no. 5, pp. 590 - 603, 2003.

[22] Y. Dong and J. Ma, "Contourlet-based texture calssification with product Bernoulli distribution," Lecture Notes in Computer Science, vol. 6676, pp. 9 - 18, 2011.

[23] T. Ojala, M. Pietikainen and T. Maenpaa, "Multiresolution gray-scale and rotation invariant texture classification with local binary patterns," IEEE Transactions on Pattern Analysis and Machine Intelligence, vol. 24, no. 7, pp. 971 - 984, 2002.

[24] S. Liao, M. W. K. Law and A. C. S. Chung, "Dominant local binary patterns for texture classification," IEEE Transaction on Image Processing, vol. 18, no. 5, pp. 1107-1118, 2009.

[25] Z. Guo, L. Zhang and D. Zhang, "A completed modeling of local binary pattern operator for texture classification [J]," IEEE Transaction on Image Process, vol. 19, no. 6, pp. 1657-1663, 2010.

[26] J. Li, S. Fan, Z. Wang, H. Li and C. C. Chang, "An optimized CLBP descriptor based on a scalable block size for texture classification," KSII Transactions on Internet and Information Systems, vol. 11, no. 1, pp. 288-301, 2017.

[27] X. Y. Tan and B. Triggs, "Enhanced local texture feature sets for face recognition under difficult lighting conditions [J]," IEEE Transaction on Image Processing, vol. 19, no. 6, pp. 168 - 182, 2007.

[28] J. Yang, Y. Jiao, N. Xiong and D. Park, "Fast face gender recognition by using local ternary pattern and extreme learning machine," KSII Transactions on Internet and Information Systems, vol. 7, no. 7, pp. 1705-1720, 2013.

[29] Z. Yang, D. S. Huang and J. Wei, "Completed local binary count for rotation invariant texture classification," IEEE Transactions on Image Processing, vol. 21, no. 10, pp. 4492-4497, 2012.

[30] Y. Dong and J. Ma, "Bayesian texture classification based on contourlet transform and BYY harmony learning of Poisson mixtures," IEEE Trans Image Process, vol. 21, no. 3, pp. 909-918, 2012.

[31] Y. Dong, D. Tao, X. Li, J. Ma and J. Pu, "Texture classification and retrieval using shearlets and linear regression," IEEE Transactions on Cybernetics, vol. 1, no. 99, pp. 1, 2014.

[32] X. Tan and B. Triggs, "Enhanced Local Texture Feature Sets for Face Recognition Under Difficult Lighting Conditions," IEEE Transactions on Image Processing, vol. 19, no. 6, pp. 1635-1650, 2010.